A time-domain approach to the extinction paradox for scattering of electromagnetic waves

Mats Gustafsson, Christian Sohl, Anders Karlsson, and Gerhard Kristensson
Dept. of Electrical and Information Technology, Lund University, P.O. Box 118, S-221 00 Lund, Sweden.
{Mats.Gustafsson, Christian.Sohl, Anders.Karlsson, Gerhard.Kristensson}@eit.lth.se; fax +46-46 12 99 48.

Abstract

The extinction paradox states that a perfectly electric conducting target which is large compared to the wavelength removes from the incident radiation exactly twice the amount of power it can intercept by its geometrical cross section area. In this paper, the extinction paradox is generalized to include temporally dispersive material parameters with finite values of the permittivity and the permeability. From a time-domain approach it is shown that the high-frequency limit of the extinction cross section depends on the material parameters of the target and that a limiting value not necessarily exists. These findings are exemplified by several numerical illustrations with different values of the extinction cross section in the high-frequency limit.

1 Introduction

The extinction paradox states that, in the high-frequency regime, a perfectly electric conducting (PEC) target removes exactly twice the amount of energy it can intercept by its geometrical cross section area [1–3]. Here, the paradoxical character lies in the fact that the effective cross section area becomes twice as large as one would expect from the geometrical optics approximation. For a PEC sphere of radius a, this means that the extinction cross section (*i.e.*, the sum of the scattering and absorption cross sections) approaches $2\pi a^2$ as the wavelength of the incident radiation becomes much smaller than a, *cf.*, the limiting value of the Mie series in Ref. 3. A common explanation for the high-frequency contribution to the extinction cross section, besides the geometrical cross section area due to a direct removal of energy from the incident radiation, is that the additional effect originates from diffraction phenomena or small-angle scattering. This explanation is presented in Refs. 1 and 4 as a result of Babinet's principle and scalar diffraction theory. However, the use of Babinet's principle is unsatisfactory in many ways, *e.g.*, numerical illustrations in this paper indicate that the high-frequency limit of the extinction cross section may very well be oscillatory and thus not well-defined. Another common approach to the extinction paradox of convex targets is based on the physical optics approximation which correctly reproduces twice the geometrical cross section area in the high-frequency limit.

The analysis of the extinction paradox in Refs. 1 and 2 is also restrictive since it does not apply to penetrable targets with finite values of the permittivity and the permeability. In contrast to the many frequency domain approaches found in the literature, this paper investigates the extinction paradox using time-domain ideas discussed in Ref. 5. In particular, this paper shows that for a large class of targets with temporally dispersive material parameters, the extinction cross section does not approach twice the geometrical cross section area in the high-frequency limit. Instead, the results suggest that the extinction paradox depends on the high-frequency behavior of the chosen material models. The study of the extinction paradox is motivated by a new theory for broadband scattering of electromagnetic waves set forth in Ref. 6. Numerical results also support the conclusion by L. Brillouin in Ref. 4 that the extinction paradox "*…is of such general character that it must certainly apply to a variety of similar problems in acoustics and wave mechanics*".

2 The extinction paradox as a result of energy conservation

Consider a bounded target in an otherwise empty space with vacuum. An incident plane pulse propagating in the $\hat{\boldsymbol{k}}$-direction is given by $\boldsymbol{E}_{\rm i}(\boldsymbol{x},t) = \sqrt{\epsilon_0}\hat{\boldsymbol{e}} f(t - \hat{\boldsymbol{k}}\cdot\boldsymbol{x}/{\rm c}_0)$, where $f(\tau') = 0$ for $\tau' < 0$, and $\tau' > \tau$ and η_0 and ${\rm c}_0$ denote the wave impedance and phase velocity of free space, respectively. Let a circular cylinder of finite length with the $\hat{\boldsymbol{k}}$-axis as symmetry axis and surface ∂V with outward-directed normal unit vector $\hat{\boldsymbol{n}}$ circumscribe the target such that the object does not touch the cylinder. The projection of the target on the bottom surface of the cylinder is denoted by $\mathcal{A}$ and has the area A, see Fig. 1. Decomposed the total electric field into an incident and a scattered field according to $\boldsymbol{E}(\boldsymbol{x},t) = \boldsymbol{E}_{\rm i}(\boldsymbol{x},t) + \boldsymbol{E}_{\rm s}(\boldsymbol{x},t)$.

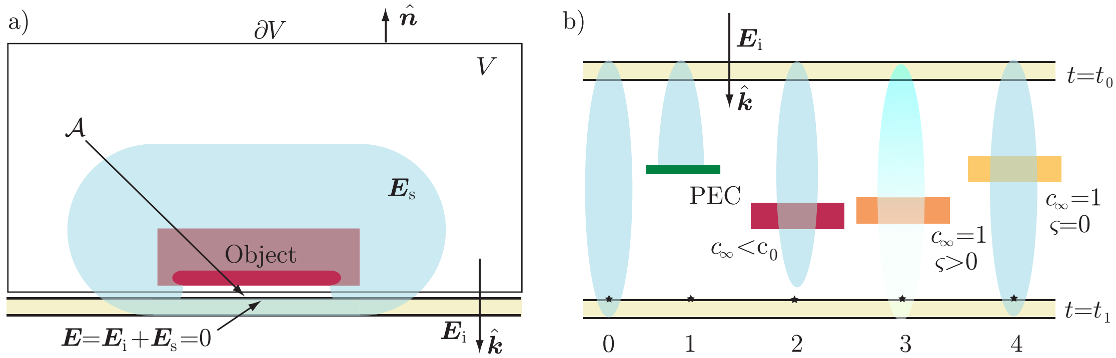

Figure 1: a) The temporal and spatial support of the scattered and incident fields for an object with a phase velocity $c_\infty < \mathrm{c}_0$. b) Illustrations of the shadow regions for various scattering targets.

The extincted energy is the sum of the absorbed and scattered energies at a sufficiently large time ($t = \infty$)

$$-\int_{\mathbb{R}}\int_{\partial V}\big(\boldsymbol{E}(\boldsymbol{x},t)\times\boldsymbol{H}(\boldsymbol{x},t)-\boldsymbol{E}_\mathrm{s}(\boldsymbol{x},t)\times\boldsymbol{H}_\mathrm{s}(\boldsymbol{x},t)\big)\cdot\hat{\boldsymbol{n}}(\boldsymbol{x})\,\mathrm{dS}\,\mathrm{d}t = -\int_{\mathbb{R}}\int_{\partial V}\big(\boldsymbol{E}_\mathrm{i}(\boldsymbol{x},t)\times\boldsymbol{H}_\mathrm{s}(\boldsymbol{x},t)+\boldsymbol{E}_\mathrm{s}(\boldsymbol{x},t)\times\boldsymbol{H}_\mathrm{i}(\boldsymbol{x},t)\big)\cdot\hat{\boldsymbol{n}}(\boldsymbol{x})\,\mathrm{dS}\,\mathrm{d}t \quad (1)$$

Causality ensures that when the pulse width goes to zero, $\tau \to 0$, the support of the incident and scattered fields can only overlap at the planar surface $\mathcal{A}$ with outward-directed unit normal vector $\hat{\boldsymbol{n}} = \hat{\boldsymbol{k}}$. This simplifies (1) to

$$W_\mathrm{ext} = -\mathrm{c}_0 \lim_{\tau\to 0}\int_{\mathbb{R}}\int_{\mathcal{A}} \mu_0 \boldsymbol{H}_\mathrm{i}(\boldsymbol{x},t)\cdot\boldsymbol{H}_\mathrm{s}(\boldsymbol{x},t)+\epsilon_0\boldsymbol{E}_\mathrm{s}(\boldsymbol{x},t)\cdot\boldsymbol{E}_\mathrm{i}(\boldsymbol{x},t)\,\mathrm{dS}\,\mathrm{d}t. \quad (2)$$

Define the short pulse extinction cross section as the quotient between the extincted energy and the incident energy flux, *i.e.*,

$$\Sigma_\mathrm{ext} = \frac{W_\mathrm{ext}}{\mathrm{c}_0\int_{\mathbb{R}}|f(\tau')|^2\,\mathrm{d}\tau'} = 2A - \lim_{\tau\to 0}\frac{\int_{\mathbb{R}}\int_{\mathcal{A}}\epsilon_0\boldsymbol{E}(\boldsymbol{x},t)\cdot\boldsymbol{E}_\mathrm{i}(\boldsymbol{x},t)+\mu_0\boldsymbol{H}_\mathrm{i}(\boldsymbol{x},t)\cdot\boldsymbol{H}(\boldsymbol{x},t)\,\mathrm{dS}\,\mathrm{d}t}{\int_{\mathbb{R}}|f(\tau')|^2\,\mathrm{d}\tau'}. \quad (3)$$

The short pulse extinction cross section depends on the geometry of the target and its material parameters. Here, an isotropic non-magnetic material is considered with a the time-domain constitutive relation given by $\boldsymbol{D} = \epsilon_0(\epsilon_\infty\boldsymbol{E} + \chi * \boldsymbol{E})$, where $\chi(t)$ denotes the susceptibility kernel and $*$ denotes temporal convolution. The corresponding frequency domain relations are quantified by the permittivity $\epsilon(\omega)$, where ω denotes the angular frequency. The following four important special cases as illustrated in Fig 1:

1. The target is perfectly electric conducting (PEC). In this case $\boldsymbol{E}\cdot\boldsymbol{E}_\mathrm{i} = 0$ and $\boldsymbol{H}\cdot\boldsymbol{H}_\mathrm{i} = 0$ when $\boldsymbol{x}\in\mathcal{A}$ and hence $\Sigma_\mathrm{ext} = 2A$.

2. The target is a dielectric material with an optical response $\epsilon_\infty > 1$. The wave front travels with the phase velocity $c_\infty = \mathrm{c}_0/\sqrt{\epsilon_\infty}$ in the target implying that $\boldsymbol{E}\cdot\boldsymbol{E}_\mathrm{i} = 0$ and $\boldsymbol{H}\cdot\boldsymbol{H}_\mathrm{i} = 0$ when $\boldsymbol{x}\in\mathcal{A}$. Hence $\Sigma_\mathrm{ext} = 2A$.

3. The object is a dispersive medium with phase velocity $c_\infty = \mathrm{c}_0$ and $\chi(0) > 0$, or equivalently $\epsilon(\omega) = 1 - \mathrm{i}\varsigma/\omega + \mathcal{O}(\omega^{-2})$ as $\omega\to\infty$, where $\varsigma = 1/\chi(0)$, *cf.*, the Debye and conductivity models. The wave front travels with the speed c_0 but is attenuated. One can show that the shape of the wave front is unaffected by the object but that attenuated by a factor of $\exp(-\chi(0)\Delta\ell/2\mathrm{c}_0)$ when it travels a distance $\Delta\ell$ in the medium. Thus $0 < \boldsymbol{E}_\mathrm{i}\cdot\boldsymbol{E} < |\boldsymbol{E}_\mathrm{i}|^2$ when $\boldsymbol{x}\in\mathcal{A}$ and hence $0 < \Sigma_\mathrm{ext} < 2A$.

4. The object is a dispersive medium with phase velocity $c_\infty = \mathrm{c}_0$ and $\chi(0) = 0$, or equivalently $\epsilon(\omega) = 1 + \mathcal{O}(\omega^{-2})$ as $\omega\to\infty$, *cf.*, the Lorentz model. In this case the wave front is not affected by the medium and hence $\Sigma_\mathrm{ext} = 0$.

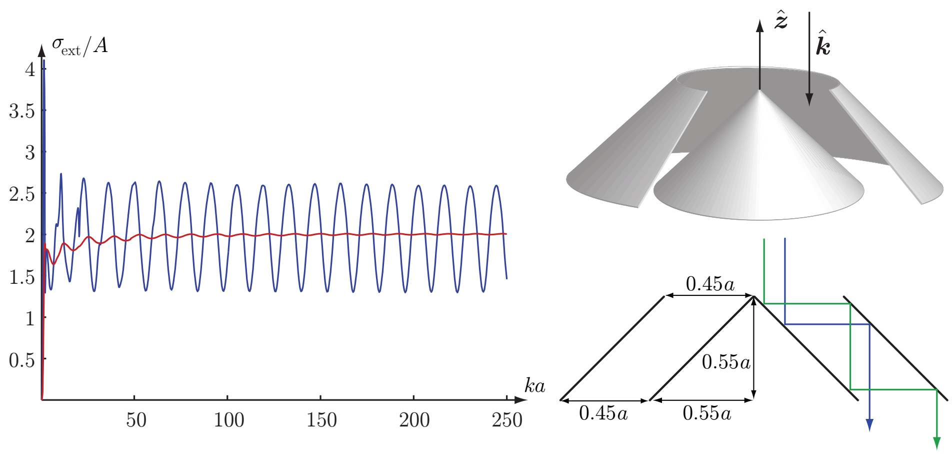

Figure 2: The extinction cross section and running averages extinction cross section in units of the geometrical cross section area $A = \pi a^2$ for the PEC geometry depicted on the right hand side.

The first two cases are the time domain (or short pulse) analogy of the extinction paradox, *i.e.*, the energy an object absorbs and scatters is twice the amount that it intercepts by its geometrical cross section area. It is illustrative to relate the time-domain extinction paradox to the corresponding high-frequency version. Fourier synthesis of the short pulse extinction cross section is

$$\Sigma_{\text{ext}}(\hat{\boldsymbol{k}}, \hat{\boldsymbol{e}}) = \lim_{\tau \to 0} \frac{\int_0^\infty \sigma_{\text{ext}}(\omega; \hat{\boldsymbol{k}}, \hat{\boldsymbol{e}}) |g(\omega)|^2 \, \mathrm{d}\omega}{\int_0^\infty |g(\omega)|^2 \, \mathrm{d}\omega}, \tag{4}$$

where σ_{ext} denotes the extinction cross section and $g(\omega)$ is the Fourier transform of $f(t)$. Although, the derivation is based on a finite pulse width, it can be generalized, giving

$$\Sigma_{\text{ext}}(\hat{\boldsymbol{k}}, \hat{\boldsymbol{e}}) = \lim_{\omega \to \infty} \frac{1}{\omega} \int_0^\omega \sigma_{\text{ext}}(\omega'; \hat{\boldsymbol{k}}, \hat{\boldsymbol{e}}) \, \mathrm{d}\omega', \tag{5}$$

where it is seen that the running average of the extinction cross section approaches Σ_{ext} in the high frequency limit. The extinction paradox then reads: *in the high frequency limit, on average the absorbed and scattered power of an object is less then or equal to twice the power that it can intercept by its geometrical cross section area*, where equality holds for objects with phase velocity $c_\infty < c_0$.

3 Numerical examples

Numerical results for a truncated cone with a displaced top, dielectric sphere, and temporal dispersive layered sphere are used to illustrate the high-frequency limit of the extinction cross section, running average extinction cross section, and the short pulse extinction cross section.

The truncated cone with a displaced top is illuminated by a plane wave incident along the symmetry axis, as depicted in Fig. 2. The object is PEC and has a geometrical cross section area $A = \pi a^2$ for $\hat{\boldsymbol{k}} = -\hat{\boldsymbol{z}}$. The extinction cross section is determined with a MoM code for $1 \leq ka \leq 250$. A simple geometrical optics analysis suggests that it is only the rays that are reflected between the conical surfaces that can contribute to the forward scattering. These rays are phase shifted causing a constructive and destructive interference pattern in the forward scattering, and, hence, an oscillatory extinction cross section. Note that the oscillation frequency $ka \approx 14 \approx 2\pi/0.45$ is consistent with the geometrical optics approximation. It is observed that high frequency limit of the extinction cross section does not exist. Moreover, σ_{ext} does not simple oscillate symmetrically around $2A$. However, the running average (5) of the extinction cross section approaches $2A$.

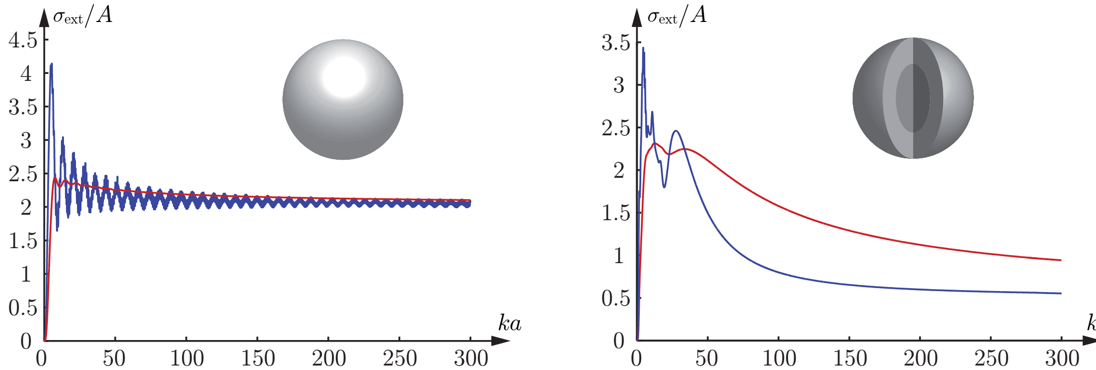

Figure 3: The extinction cross section in units of the geometrical cross section area $A = \pi a^2$ for a sphere of radius a. The left figure represents a homogeneous sphere with a constant permittivity $\epsilon = 2$ while the right figure is for a stratified sphere with a Lorentz dispersive media in the outermost layer. The corresponding running average extinction cross sections are illustrated by the smoothly varying curves.

The extinction cross section of a dielectric sphere with a constant permittivity $\epsilon = 2$ is depicted to the left in Fig. 3. It is observed that $\sigma_{\rm ext}$ oscillates around $2A$ and that the amplitude of the oscillations decreases with ka. The corresponding running averages extinction cross section (5) is given by the smooth curve that slowly approaches $2A$. A stratified sphere with a PEC core (with radius $a/2$) surrounded by a Lorentz dispersive media is illustrating the effect of temporal dispersion on the short pulse extinction cross section. The Lorentz model is given by $\epsilon(\kappa) = 1 - \kappa_{\rm p}^2/(\kappa^2 - \kappa_0^2 + {\rm i}\kappa\nu)$, where $\kappa = ka$, $\kappa_0 = \kappa_{\rm p} = 10$, and $\nu = 0.1\kappa_0$. It is observed that $\sigma_{\rm ext}$ approaches $A/2$ as $ka \to \infty$ in the right hand side of Fig. 3. This agrees with the general result as the wave front is unaffected by the Lorentz medium giving a shadow region defined by the projection of the PEC core. The convergence of the running average extinction cross section is seen to converge slower.

4 Conclusions

The time domain approach offers new insights into the underlying physics of the extinction paradox. In contrast to the classical frequency domain explanations, the new approach is solely based on energy conservation and causality and does not utilize either scattering theory nor high-frequency approximations. A short pulse extinction cross section is defined and shown to be bounded by twice the geometrical cross section area of the object. Moreover, it is shown that the running average of the high-frequency extinction cross section approaches the short pulse extinction cross section in the high frequency limit.

References

[1] H. van de Hulst. *Light Scattering by Small Particles*. New York: John Wiley & Sons, Inc., 1957.

[2] C. F. Bohren and D. R. Huffman. *Absorption and Scattering of Light by Small Particles*. New York: John Wiley & Sons, 1983.

[3] R. G. Newton. *Scattering Theory of Waves and Particles*. New York: Dover Publications, 2nd edn., 2002.

[4] L. Brillouin. “The scattering cross section of spheres for electromagnetic waves”. *Appl. Phys.*, vol. 20, pp. 1110–1125, 1949.

[5] A. Karlsson. “On the time domain version of the optical theorem”. *Am. J. Phys*, vol. 68(4), pp. 344–349, 2000.

[6] C. Sohl, M. Gustafsson, and G. Kristensson. “Physical limitations on broadband scattering by heterogeneous obstacles”. *J. Phys. A: Math. Theor.*, vol. 40, pp. 11165–11182, 2007.